Effect of vanadium on microstructure and wear behaviour of Fe based C–B–Ni hardfacing alloy

L. Rovatti*[1], R. Casati[1], A. Emami[1], N. Lecis[1], O. Stejskal[2], C. Andrianopoli[3] and M. Vedani[1]

Introduction

Hardfacing is a widely diffused strategy to improve surface properties of tools and plant equipment by the deposition of a material layer aimed at improving surface wear and corrosion resistance without significant changes of ductility and toughness of the substrate.[1] This method can be used to produce deposits having thickness up to the millimetre scale, by cladding based technologies (e.g. laser deposition, plasma torch arc cladding) or by casting based processes (e.g. spin casting).

The wear resistance of the coating can be significantly improved by promoting a dispersion of hard phases in the microstructure. Hence, Fe based hardfacing alloys usually rely on copious precipitation of primary and secondary carbides based on strong carbide-forming elements like Ti, W, Mo, Cr, Nb and V.[2–6] Distribution and size of secondary carbides also have a great influence on wear resistance of steels. In particular, the hardness can be increased by the formation of a fine dispersion of secondary carbides in a relatively ductile and tough matrix such as tempered martensite.[7] When high wear resistance properties are required, also the toughness of the carbides has to be considered to prevent premature failure of these phases.[8] Hardfacing alloys with a combination of hard and tough carbides showed very high abrasive wear resistance since tough phases can sustain higher loads and service times before failure occurs under the action of the abrasive environment.[1] In particular, it has been shown that V is a strong carbide-forming element, producing MC type phases characterised by high hardness.[9,10] It was also stated that V has a high solubility in α-Fe solid solution and in other M_3C and M_7C_3 carbides.[5,11] Moreover, limited amounts of V in Fe–Cr–C alloys, revealed to have relatively low effects on the solidification behaviour.[5]

In this paper, a standard Fe–C–B–Ni hardfacing alloy in the form of powder was blended with increasing amount of Fe–V rich powders and cast in alumina crucible in order to analyse the relationship between chemistry, microstructure, solidification behaviour and properties such as hardness and wear behaviour of the new experimental alloys.

Materials and experimental procedures

The reference material was a commercial Fe based C–B–Ni abrasion resistant powder alloy with the chemical composition reported in Table 1 and a particle size in the range 45–355 μm. Batches of the reference alloy were blended with several additions: 5, 10, 20, 30 and 40 wt-% of an atomised Fe–12V–Cr alloy powder (particle size in the range 50–150 μm), whose composition is given in Table 1. Both starting powders are characterised by an

[1]Politecnico di Milano, Dipartimento di Meccanica, Milan, Italy
[2]Bernex Bimetallic Sro, Modrice Bei Brno, Czech Republic
[3]Cogne Acciai Speciali Spa, Aosta, Italy

*Corresponding author, email ludovica.rovatti@polimi.it

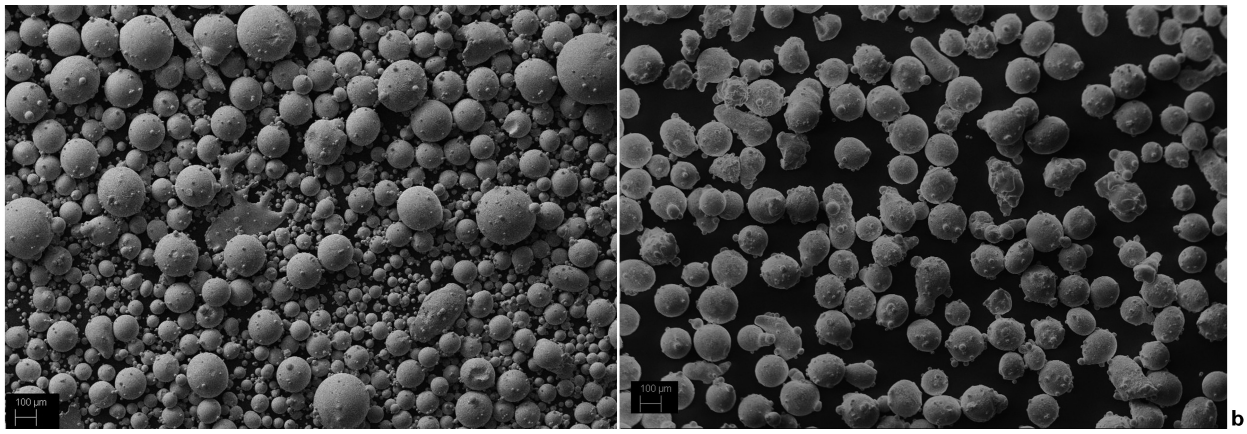

1 *a* micrograph (SEM) of reference Fe–C–B–Ni (V0) alloy powder and *b* SEM image of Fe–12V–Cr powder used in casting experiments

almost spherical shape as shown in Fig. 1. The new V-bearing alloys were thus designed to reach nominal V concentrations ranging from about 0.6 up to about 4.9 wt-% as described in Table 2.

After blending the powder mixtures, the materials were placed in alumina crucibles of size $70 \times 14 \times 10$ mm or in cylindrical crucibles having diameter of 25 mm and height of 20 mm. Melting was performed in a furnace equipped with a flow of Ar as shielding gas. Differential scanning calorimetry (DSC, Setaram Instrumentation) was used to investigate the melting, solidification and solid state phase transformations of the alloys. Differential scanning calorimetry thermograms were generated by imposing a heating ramp up to 1250°C at a rate of 30°C min^{-1}, 15 min holding at maximum temperature followed by a cooling step at the same rate. In particular, the heat flow was recorded as a function of temperature and by analysing the cooling curves, the offset and onset points of the melting and solidification ranges were determined. X-ray diffraction analyses were performed to identify alloy phases found after solidification. X-ray diffraction measurements were carried out by a PANalitical X-Pert PRO instrument, with a θ–θ configuration, equipped with a RTMS X'Celerator sensor. Cu K_α (λ=0.15418 nm) radiation was employed to perform the tests. Microstructural investigations were carried out after metallographic polishing and etching with a solution of Nital 3%, by optical microscopy and scanning electron microscopy (SEM). Preliminary analyses revealed that, for the investigated cooling rates, the microstructure of samples cast in the two types of crucibles was fully comparable. Energy dispersive spectrometer was also adopted to characterise the chemistry of phases.

Macrohardness tests were carried out using a Vickers equipment with a load of 981 N while microhardness was performed by a Vickers indenter with loads of 0.49 and 0.981 N depending on the size of the phases to be measured. Wear tests were carried out on sectioned samples (cast in the larger cylindrical crucibles) using a pin-on-disc tribometer (TRB, CSM Instruments) with an alumina ball (diameter of 6 mm) as a pin, at linear sliding speed of 0.1 m s^{-1} along a circular path of about 7 mm in diameter. A normal load of 5 N was used for about 14 000 cycles, corresponding to a sliding distance of 300 m. Wear tracks were observed by SEM and their profiles were measured using a contact profilometer from which the volume loss was determined.

Table 1 Chemical compositions (wt-%) of reference Fe–C–B–Ni alloy (V0) and of Fe–12V–Cr powder

	C+B	Si	Mn	Cr	Ni	Mo	V	Fe
Fe–C–B–Ni (V0)	4.3	2.06	0.54	0	3.93	0	0	Balance
Fe–12V–Cr	2.8	0.9	0.5	5.2	0.6	1.25	12.2	Balance

Results and discussion

Solidification behaviour and microstructure

In the Fe–C–B–Ni reference alloy (V0) was observed the presence of coarse columnar primary Fe carbides/borides of the type $Fe_3(C,B)$, a limited amount of graphite, both in globular and flake-like morphologies and α-Fe + $Fe_3(C,B)$ lamellar eutectic. In addition, small amounts of Fe-rich solid solution close to the graphite phase was detected (Fig. 2).

The addition of increasing amounts of Fe–V powder led to the microstructures depicted in Fig. 3. It can be inferred that alloys V1, V2 and V3, with an addition of Fe–12V–Cr powder to the base alloy up to 20% and a V content up to 2.44%, featured an hypereutectic microstructure while higher V-rich powder additions promoted the shift to an hypoeutectic microstructure, as shown in Fig. 3*g–l*. In these latter images, the globular dark features observed at low magnification represent dendrite branches intersecting the section plane of the sample.

The XRD spectra of alloys V0, V3 and V5 are reported in Fig. 4. The XRD spectrum of the base alloy V0 confirms the presence of the oriented orthorhombic $Fe_3(C,B)$ phase, α-Fe and α'-martensite. The preferential orientation of the primary carbides/borides in the base alloy can be related to a directional solidification occurred during casting (Fig. 2*a*).

Table 2 Compositions (wt-%) of experimental high V alloys (balance Fe)

Alloy code	C+B	Si	Mn	Cr	Ni	Mo	V
V1	4.22	2.00	0.54	0.26	3.76	0.06	0.61
V2	4.15	1.94	0.54	0.52	3.60	0.13	1.22
V3	4	1.83	0.53	1.04	3.26	0.25	2.44
V4	3.85	1.71	0.53	1.56	2.93	0.38	3.66
V5	3.7	1.60	0.52	2.08	2.60	0.50	4.88

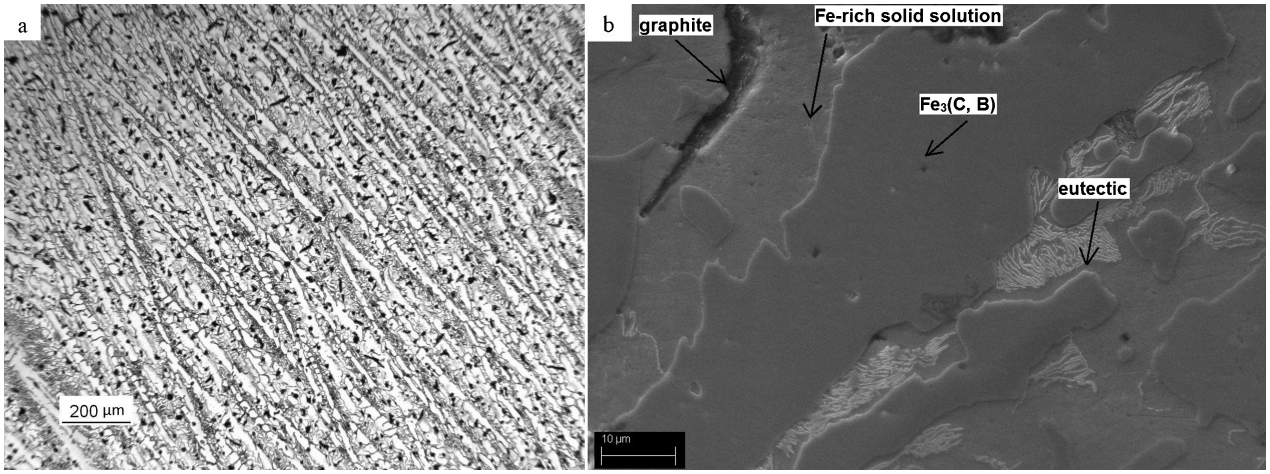

a optical micrograph; *b* detail of microstructure shown by higher magnification SEM image

2 Representative micrographs of Fe–C–B–Ni reference alloy (V0)

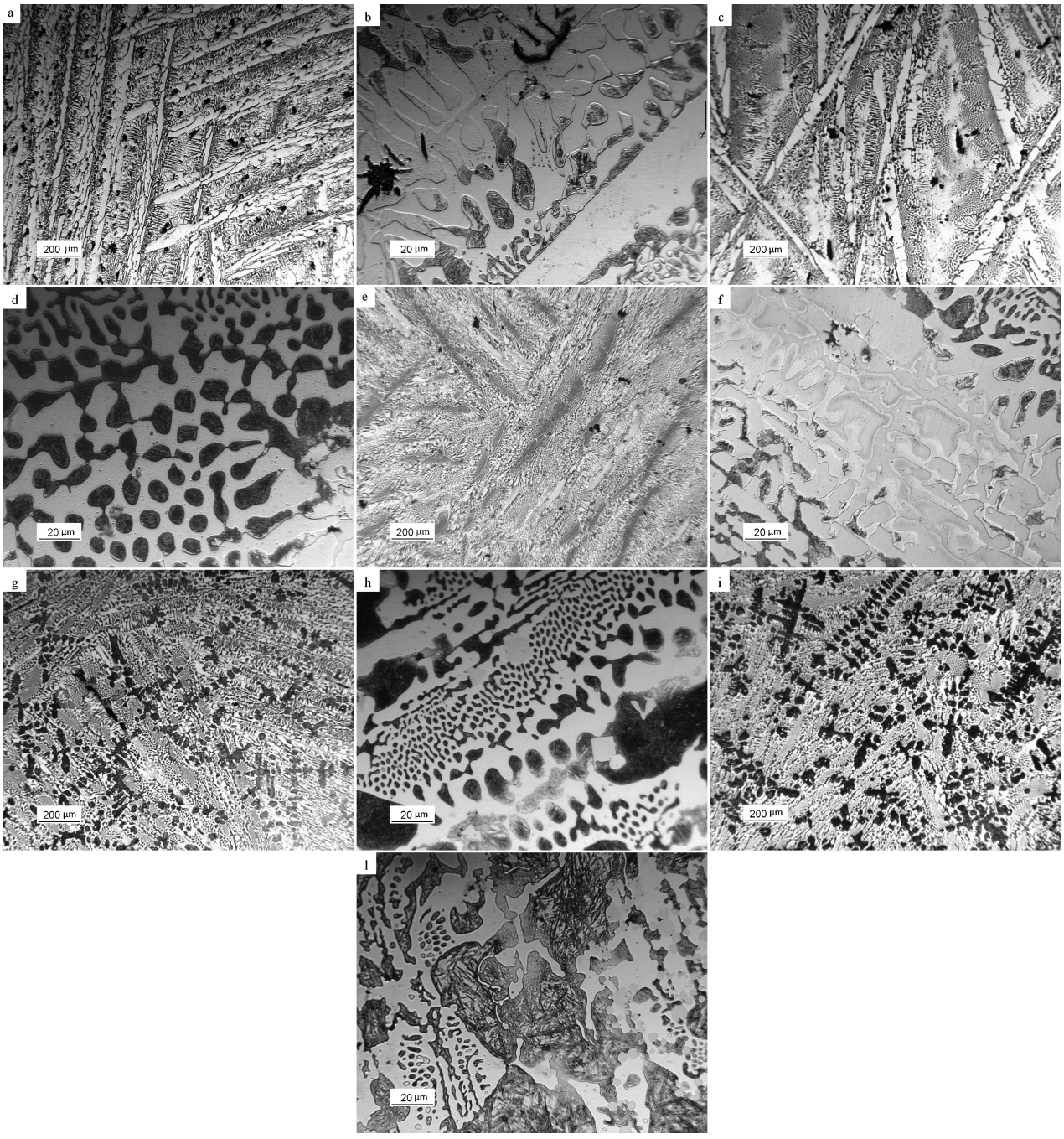

a, *b* V1; *c*, *d* V2; *e*, *f* V3; *g*, *h* V4; *i*, *l* V5

3 Representative micrographs taken at two different magnifications of alloys

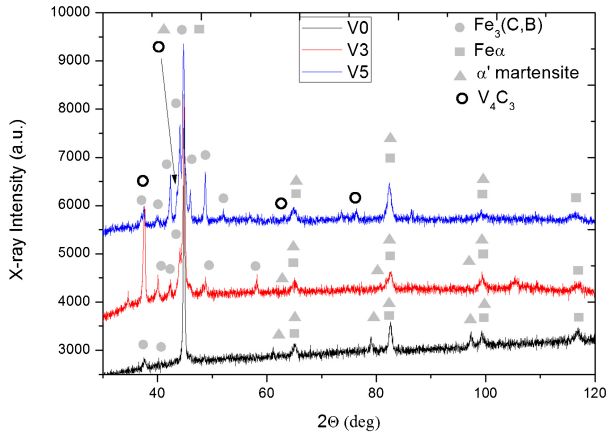

4 Spectra (XRD) of investigated alloys V0, V3 and V5

In the near eutectic and the hypoeutectic alloys V3 and V5 a more random orientation of the $M_3(C,B)$ phase was observed by XRD. In the same high V alloys it was identified the presence of a bainitic–martensitic structure depicted also by optical observations (Fig. 3*f* and *l*). Moreover, in the alloy V5 the peaks of the V_4C_3 carbides have been identified (Fig. 4).

From combined analyses of XRD data and microstructure observation, it can be stated that in the high V hypereutectic alloys (V1, V2 and V3), the primary Fe-rich carbides/borides were less homogeneously oriented and they were found in lower amount than in the corresponding base alloy. As expected, a higher content of the eutectic structure was formed when Fe–V rich powders were progressively added (compare Fig. 3*a–e*). It is therefore suggested that vanadium contributed to promote the formation of the eutectic, decreasing the primary carbide fraction and the graphite content. This observation is in agreement with the results obtained by Qi *et al*., who demonstrated by thermodynamic calculations that the eutectic composition shifted to higher C concentrations for higher V additions.[12] As confirmed by XRD, a bainitic–martensitic structure was observed in the Fe-rich phase of the eutectic fraction found in the hypereutectic alloys (see Fig. 3*b–f*) and in the primary phase of the hypoeutectic V4 and V5 alloys (see Fig. 3*l*). In the near-eutectic (V3) and hypoeutectic compositions (V4 and V5) further presence of small V-rich carbides was detected.

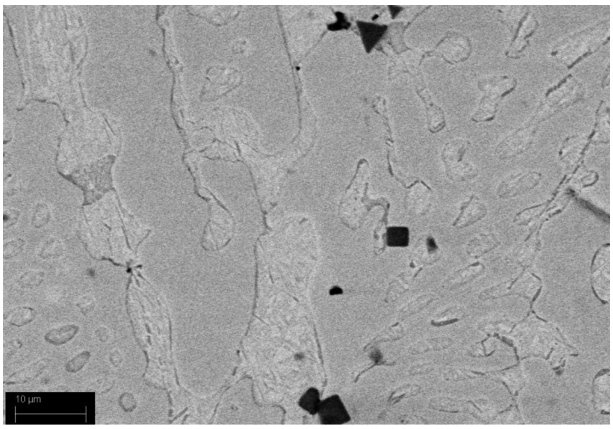

5 Micrograph (SEM) collected by backscattered electron signal of alloy V3. Blocky shaped phases are V-rich carbides

In the alloy V3, these carbides had a blocky shape with a size of a few micrometers, as shown in Fig. 5. By increasing the Fe–12V–Cr content up to 30 wt-%, a combination of cubic and spherical morphologies of the V-rich carbides was observed within a hypoeutectic composition (see Fig. 3*h*). In the hypoeutectic alloy V5 the presence of almost spherical V_4C_3 carbides with an average size of 5 µm that had nucleated close to (or as part of) the eutectic carbides was observed, as shown in Fig. 6.

The reference Fe–C–B–Ni alloy and the alloys V3 and V5 have been analysed by DSC in order to verify the possible influence of V on the melting and solidification behaviour. These two alloys were selected for the DSC analysis and pin-on-disc tests because they showed the most significant microstructures among the new V-bearing alloys. In fact, it was only possible to detect microsize V-rich particles in the alloys containing more than 10 wt-% of Fe–12V–Cr, hence, starting from the near-eutectic alloy V3 (see Fig. 5). Moreover, for the highest Fe–12V–Cr addition, corresponding to the alloy V5, the structure shifted to a fully hypoeutectic composition with a homogeneous distribution of spherical V_4C_3 carbides, as shown in Fig. 6.

Figure 7 shows the DSC curves of the reference V0 alloy and of the V-rich alloys V3 and V5. Both on heating and cooling curves, two main peaks are

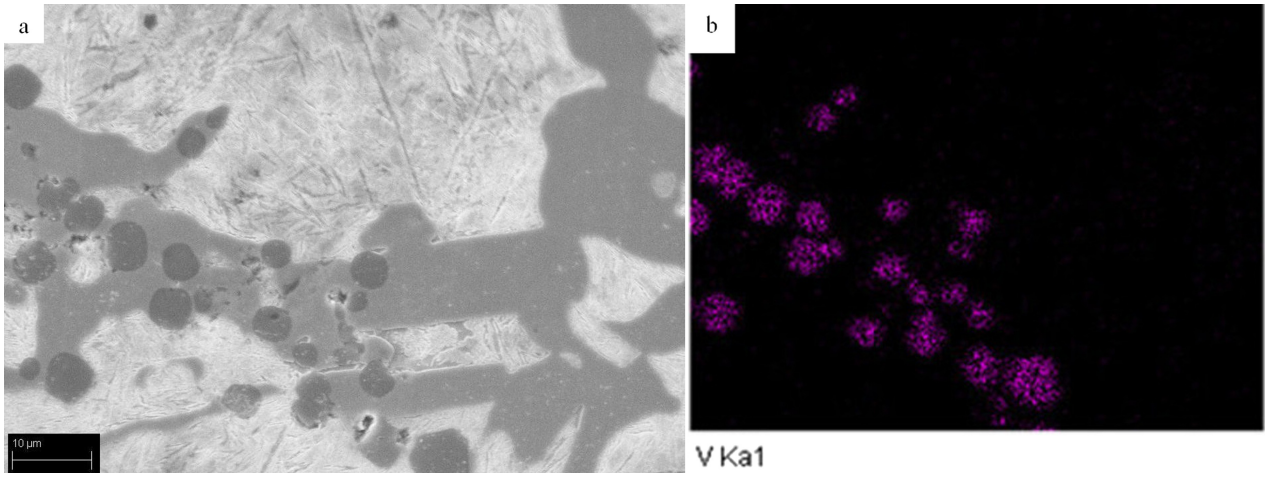

6 *a* SEM micrograph and *b* V chemical map of V-rich carbides detected in alloy V5

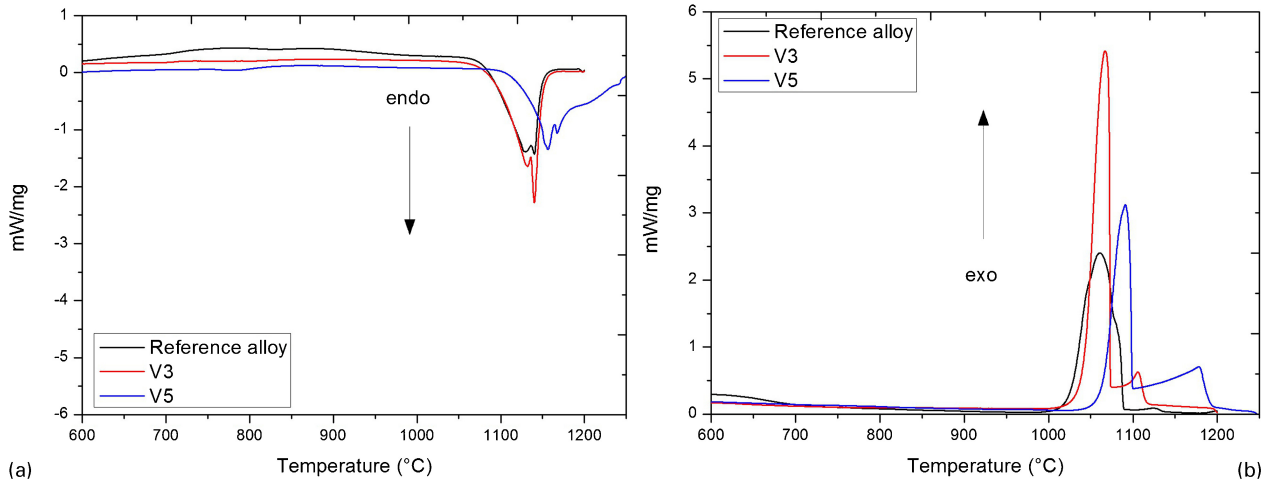

7 *a* heating and *b* cooling curves of reference V0 alloy and of V-rich alloys V3 and V5

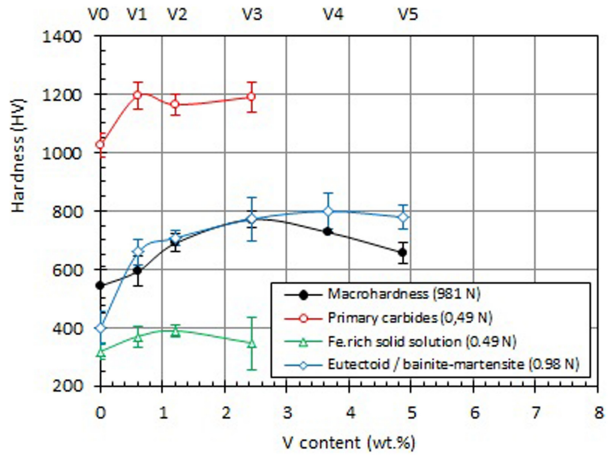

8 **Vickers hardness evolution of investigated cast alloys as a function of V content. Open symbols refer to microhardness (applied load in brackets), full symbols to macrohardness**

observed. The first peak at higher temperature is supposed to be related to the formation/dissolution of the primary phases, $M_3(C,B)$ carbides/borides in case of reference V0 alloy and alloy V3, Fe-rich solid solution for the V5 alloy. The peak at lower temperature is caused by the solidification/melting of the eutectic.

From analysis of the cooling and heating curves, the onset and offset temperatures of the solidification and melting processes were obtained. The measured values are summarised in Table 3. It is to remind that the width of solidification range is of great importance for the evaluation of solidification cracking susceptibility. It is established that the wider the solidification range, the higher the cracking probability in cast alloys.[13]

In the case of the hypereutectic alloy V3, it is inferred that the small addition of V did not increase significantly the solidification and melting ranges (ΔT) but it slightly increased the onset and offset temperatures of solidification during cooling. On the contrary, for the hypoeutectic V5 alloy, wider solidification and melting ranges were measured compared to the base alloy mainly due to the marked hypoeutectic nature of the composition.

Hardness and wear behaviour

In Fig. 8 the bulk hardness of the alloys and the microhardness measured in the different phases of the investigated alloys are plotted. As expected, the high V alloys V2, V3 and V4 resulted to be harder than the reference alloy V0. In the case of the hypoeutectic alloys V4 and V5, a decrease in hardness is observed due to the lack of contribution given by the primary carbides. However, the presence of a hard matrix and of the finer V-rich hard carbides allowed to preserve a relatively high hardness even for these alloys. From specific measurements it can be reported that the microhardness of the globular V-rich carbides was 1920 ± 342 HV. This result is consistent with the hardness value reported in literature.[10]

In the V-bearing hypereutectic alloys (samples V1, V2 and V3), improved microhardness values of the primary $M_3(C,B)$ carbides have also been recorded, probably due to the effect of V as substitutional element. A higher microhardness value of the matrix was measured in the bainitic–martensitic structure with respect to the main eutectoid structure observed in the reference alloy (Fig. 2*b*) whereas, in general, the Fe-rich solid solution was only slightly affected by the presence of V.

Alloys V3 and V5 were also considered to compare their wear behaviour with that of the reference alloy V0. In Fig. 9 three representative curves of the friction coefficient behaviour are reported as a function of the

Table 3 Melting and solidification ranges of analysed alloys

	Heating			Cooling		
Alloy	*T* onset/°C	*T* offset/°C	ΔT/°C	*T* onset/°C	*T* offset/°C	ΔT/°C
Fe–C–B–Ni (reference)	1090.1	1149.1	59	1088.2	1025.6	62.6
V3	1096.7	1149.8	53.1	1114.9	1042.5	72.4
V5	1135.6	1236	100.4	1191.6	1064.5	127.1

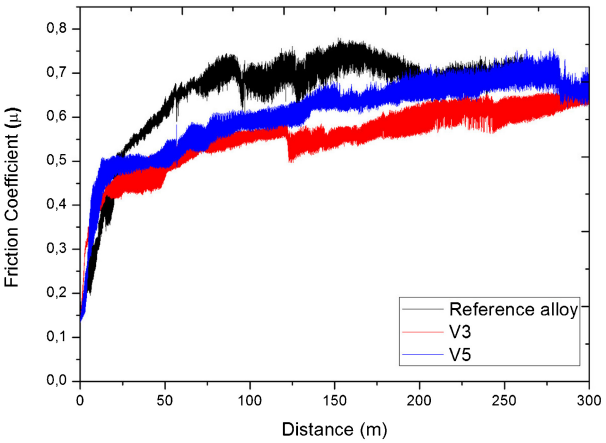

9 Evolution of friction coefficient of reference alloy (V0) and of near-eutectic (V3) and hypoeutectic (V5) V-rich alloys

sliding distance. The three alloys showed a quite similar friction coefficient evolution featuring a steady state region after about 100 m of sliding distances. A similar condition was already observed for other tested Fe–Cr–B alloys in the literature and it was explained by considering the effects of oxide layer produced during the wear process.[14]

In Table 4 the data about wear volume loss are summarised for the investigated alloys after the pin-on-disc tests at a sliding distance of 300 m. A remarkably higher volume loss was measured in the reference alloy when compared with alloys V3 and V5. The improvement led by the V addition can be estimated in 76 and 84% over the reference material for the V3 and V5 alloy, respectively.

Analyses of the wear tracks of the investigated alloys showed the presence of specific regions covered by an oxidation layer mainly rich in Fe, O and Si. Cracks were often found associated to these oxide regions, as reported in Fig. 10.

In particular, from Fig. 10*c* showing the worn surface of V5 alloy, it is noticed that the small spherical V-rich carbides are generally still embedded in the matrix and no sign of cracking or carbide pull-out is observed in the surrounding matrix.

It can therefore be supposed that the high wear performance of the V-bearing alloys could mainly be attributed to the high bulk hardness retained in these alloys and to the support to load-bearing action offered by the fine dispersion of tough V-rich carbides dispersed in the microstructure of the new alloys.

Conclusions

New V-rich Fe–C–B–Ni alloys cast in a laboratory furnace were investigated. The addition of Fe–12V–Cr powder to the reference alloy up to 20 wt-% promoted the formation of larger amount of eutectic structure,

Table 4 Volume losses after wear tests of investigated alloys

Alloy	Volume loss/ $\times 10^4 \mu m^3$
Reference Fe–C–B–Ni	1982 ± 150.6
V3	484 ± 83.1
V5	318 ± 62.8

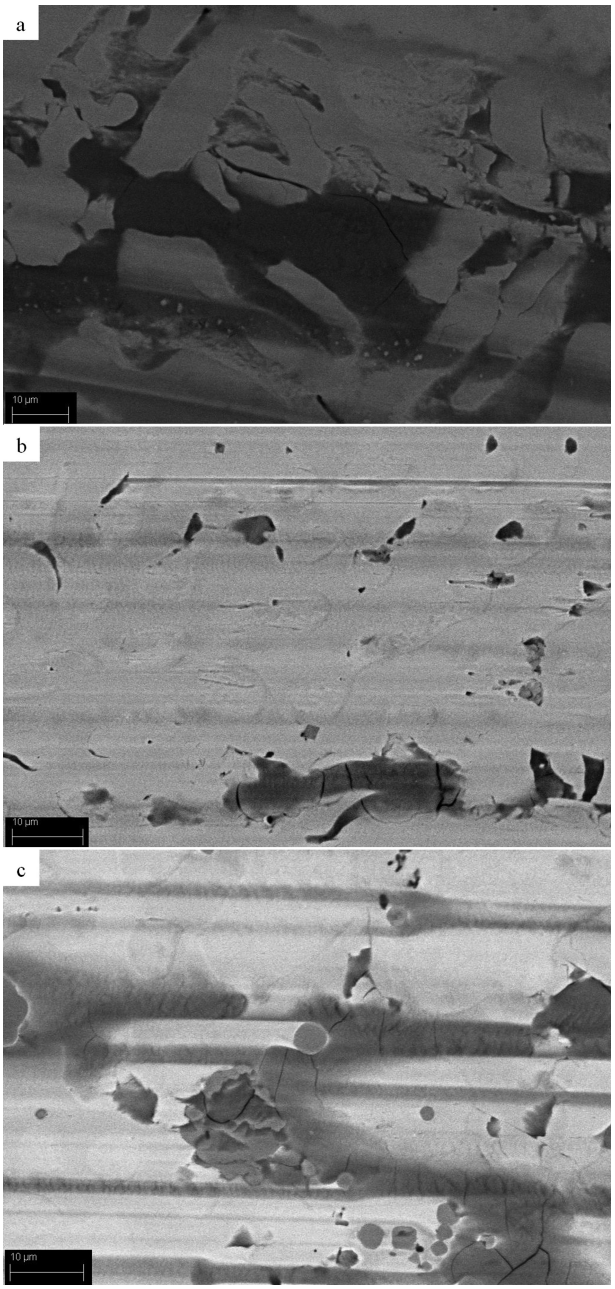

a reference alloy V0; *b* alloy V3; *c* alloy V5

10 Views (SEM) collected by backscattered electron signal of wear tracks of materials tested after sliding distance of 300 m

thus decreasing the primary carbide fraction and the graphite content as well. By increasing the Fe–12V–Cr content above 20 wt-% the V-bearing alloys assumed hypoeutectic compositions with V-rich carbides and primary dendrites characterised by a bainitic–martensitic structure. Different morphologies of vanadium carbides were observed based on the V-rich additions. In 20 wt-% of Fe–12V–Cr addition (about 2.5 wt-% of V), blocky shaped vanadium carbides with the size of a few micrometers was identified in a eutectic microstructure, whereas, for higher Fe–12V–Cr contents V_4C_3 particles with a near-spherical shape were observed within the hypoeutectic structure.

Vanadium did not significantly widen the solidification gap, at least for the hypereutectic composition,

which is a desired requisite for the limitation of solidification cracking during casting processes.

V alloying allowed increasing the hardness due to the contribution of V-rich carbides and to the conversion of the matrix into a bainitic–martensitic structure.

The high V alloys showed improved wear performance under pin-on-disc testing condition, both for hypereutectic and for hypoeutectic compositions. In particular, a decreasing of 76 and 84% of the volume loss was measured respectively for the alloys V3 and V5 compared to the reference material. In particular, it was observed that micro-size V_4C_3 carbides provide an effective load-bearing action considering that they remain embedded within the hard matrix without cracking. It can be concluded that the high wear performances of the V-bearing alloys are due to the favourable combination of distribution, size and carbide morphology in the hard matrix. Accordingly, the V-rich carbides are retained without being torn out during the pin-on-disc testing.

Acknowledgements

The present investigation was financed under the research project DEBACOAT – Development of high performance barrels with innovative gradient coatings, funded by the European Commission under the call FP7-SME-2012 (project id 315417).

The authors would like to thank Dr A. Tuissi (CNR.IENI, Italy) for XRD analyses.

References

1. M. F. Buchely, J. C. Gutierrez, L. M. Leon and A. Toro: 'The effect of microstructure on abrasive wear of hardfacing alloys', *Wear*, 2005, **259**, 52–61.
2. Q. Wang and X. Li: 'Effects of Nb, V and W on microstructure and abrasion resistance of Fe-Cr-C hardfacing alloys', *Weld. J.*, 2010, **38**, 133–139.
3. E. O. Correa, N. G. Alcantara, D. G. Tecco and R. V. Kumar: 'The relationship between the microstructure and abrasive resistance of a hardfacing alloy in the Fe-Cr-C-Nb-V system', *Metall. Mater. Trans. A*, 2007, **38A**, 1671–1680.
4. G. Azimi and M. Shamanian: 'Effect of silicon content on the microstructure and properties of Fe–Cr–C hardfacing alloys', *J. Mater. Sci.*, 2010, **45**, 842–849.
5. R. J. Chung, X. Tang, D. Y. Li, B. Hinckley and K. Dolman: 'Microstructure refinement of hypereutectic high Cr cast irons using hard carbide-forming elements', *Wear*, 2013, **301**, 695–706.
6. C.-M. Lin, H.-H. Lai, J.-C. Kuo and W. Wu: 'Effect of carbon content on solidification behaviors and morphological characteristics of the constituent phases in Cr-Fe-C alloys', *Mater. Charact.*, 2011, **62**, 1124–1133.
7. H. Leitner, R. Ebner, B. Major and G. Pockl: Proc. 5th Int. Conf. on 'Tooling', (ed. F. Jeglitsch, R. Ebner and H. Leitner), University of Leoben, Austria, 369–381; 1999.
8. C.-H. Lin, C.-M. Chang, J.-H. Chen and W. Wu: 'The effects of additive elements on the microstructure characteristics and mechanical properties of Cr-Fe-C hard-facing alloys', *J. Alloys Compd*, 2010, **498**, 30–36.
9. F. Cheng, Y. Wang and T. Yang: 'Microstructure and wear properties of Fe– VC–Cr7C3 composite coating on surface of cast steel', *Mater. Charact.*, 2008, **59**, 488–492.
10. C. Subramanian, K. N. Stratford, T. P. Wilks and L. P. Ward: 'On the design of coating systems: metallurgical and other considerations', *J. Mater. Process. Technol.*, 1996, **56**, 385–397.
11. J. J. Coronado and A. Sinatora: 'Load effect in abrasive wear mechanism of cast iron with graphite and cementite', *Wear*, 2009, **267**, 6–9.
12. X. Qi, Z. Jia, Q. Yang and Y. Yang: 'Effects of vanadium additive on structure property and tribological performance of high chromium cast iron hardfacing metal', *Surf. Coat. Technol.*, 2011, **205**, 5510–5514.
13. J. Campbell: 'Castings', 2nd edn; 2003, Oxford, Butterworth Heinemann Publisher.
14. A. A. Sorour, R. R. Chromik and M. Brochu: 'Tribology of a Fe–Cr–B-based alloy coating fabricated by a controlled short-circuit mig welding process', *Metallogr. Microstruct. Anal.*, 2013, **2**, 223–233.